

EXTREME VALUE ANALYSIS OF FLUCTUATING  
AIR LOADS ACTING ON A CYLINDER

Thesis by

Jay Chung Chen

In Partial Fulfillment of the Requirements

For the Degree of  
Aeronautical Engineer

California Institute of Technology

Pasadena, California

1967

(Submitted September 23, 1966)

## ACKNOWLEDGMENT

The author would like to express his appreciation to Dr. Y. C. Fung for his encouragement and guidance for this study, and to the National Science Foundation for providing financial assistance. A sincere thanks is given to Dr. L. V. Schmidt, Mr. R. E. Spitzer and Mr. M. E. Jessey for their very helpful advice and assistance for data handling.

ABSTRACT

The fluctuating air loads over the surface of a smooth, cantilevered circular cylinder perpendicular to a flow in the supercritical Reynolds number ranging from  $2.5 \times 10^5$  to  $7.5 \times 10^5$  have been investigated according to Gumbel's extreme value theory.

The envelope of the extreme values of the pressure was found to be much greater than the static pressure and the root-mean-square values and decreased with increasing Reynolds number.

On the other hand, the envelope of the extreme values of the resultant force was generally unrelated with Reynolds number.

## NOMENCLATURE

<u>Symbols</u>	<u>Definition</u>
$F(x)$	Probability function that the value of variate is less than a certain $x$ .
$f(x)$	Density of the probability function.
$\Phi$	Probability that the largest value falls short of $x_n$ .
$n$	Number of independent observations.
$Y$	Reduced extreme value.
$m$	The mean of a probability distribution.
$\sigma$	The standard deviation of a probability distribution.
$\alpha, u$	Parameters.
$\gamma$	Euler's constant.
$T(x)$	Return period.
$\sigma(N), \bar{Y}(N)$	Constants.
$N$	Number of batches of data.
$Re$	Reynolds number.
$C_L$	Lift coefficient
$C_D$	Drag coefficient
$C_f$	Coefficient of resultant force.
$q$	Dynamic pressure.

TABLE OF CONTENTS

TITLE	PAGE
1. INTRODUCTION	1
2. THE EXTREME VALUE THEORY	2
3. APPLICATION TO THE FLUCTUATING AIR LOAD ACTING ON A CYLINDER	5
4. ENVELOPE OF EXTREME VALUES OF PRESSURE	9
5. ENVELOPE OF EXTREME VALUES OF RESULTANT FORCE	12
6. VARIATION OF THE EXTREME VALUE INTERVAL	13
7. DISCUSSION	14
8. CONCLUSIONS	15
9. REFERENCES	16
10. WORKSHEETS	17
11. TABLES	20
12. FIGURES	22

ILLUSTRATIONS

FIGURE	PAGE
1. Probability Paper	22
2. Extreme Value Envelope of Pressure Coefficient at Re = $2.5 \times 10^5$	23
3. Extreme Value Envelope of Pressure Coefficient at Re = $3.8 \times 10^5$	24
4. Extreme Value Envelope of Pressure Coefficient at Re = $5.3 \times 10^5$	25
5. Extreme Value Envelope of Pressure Coefficient at Re = $6.5 \times 10^5$	26
6. Extreme Value Envelope of Pressure Coefficient at Re = $7.5 \times 10^5$	27
7. Extreme Value of Resultant Force	28
8. Extreme Value vs. Intervals	29
9. Initial Distribution	30

## 1. INTRODUCTION

The knowledge of fluctuating air loads for flow over a circular cylinder in the supercritical regions has engineering application to current problems of importance in dealing with the response of large cylindrical objects such as smokestacks and missiles on open launch pads. Many investigations have been made (Refs. 1, 2, 3, 4), and one important nature of the air loads that was shown in every investigation is the randomness of air loads at supercritical flow region.

For the problem of structural design based on ultimate static failure, the larger air loads are of particular interest, as they are likely to cause structural damage. As it will be shown later, the extreme air loads are much greater than the average loads. The designer would like to know how large these extreme air loads are and how often they occur. Because the larger air loads are infrequent, measurements available from limited samples of data will generally not extend to the larger and critical values of air loads. Consequently, an important problem in these investigations is the development of techniques for estimating the probabilities of encountering these larger values.

The statistical theory of extreme values which was developed by E. J. Gumbel has indicated a rational approach to the problem of predicting the probability of occurrence of extreme values. Throughout this report, this theory is applied.

## 2. THE EXTREME VALUE THEORY

Let  $F(x)$  be the probability that the value of the air load is less than a certain  $x$ , and let  $f(x) = F'(x)$  be the density of probability, henceforth called the initial distribution. Then the probability that  $n$  independent observations all fall short of  $x$  is evidently  $F^n(x)$ , by the rules of multiplication of independent combined events. In other words, this is the probability for  $x$  to be the largest air load among  $n$  independent observations. Let  $x = x_n$ , then

$$\Phi(x_n) = F^n(x_n) \quad (1)$$

We call  $\Phi$  the probability of extreme values, and consider

$$\phi = \Phi'(x_n) = nF^{n-1}(x_n)f(x_n) \quad (2)$$

which is a new probability distribution.

For some given initial distribution  $F(x)$ ,  $\Phi(x)$  can be solved explicitly. For example (Ref. 5), if

$$F(x) = \frac{1}{\sigma\sqrt{2\pi}} \int_{-\infty}^x e^{-(t-m)^2/2\sigma^2} dt \quad (3)$$

is a normal distribution, where  $m$  is the mean and  $\sigma$  is the standard deviation, then

$$\Phi(x) = e^{-e^{-y}} \quad (4)$$

where

$$y = \alpha(x-u) \quad (5)$$



and 
$$\frac{1}{\alpha} = \frac{\sigma}{\sqrt{2 \log n}} \quad (6)$$

$$u = m + \sigma \sqrt{2 \log n} - \sigma \frac{\log(\log n) + \log 4\pi}{2\sqrt{2 \log n}} \quad (7)$$

But in the practical cases, either the initial distribution is unknown or it is too difficult to obtain. Gumbel has shown that if the initial distribution belongs to the so-called exponential type, then the asymptotic form of the extreme value distribution (Ref. 6) is given by eqs. (4) and (5). The parameters  $\alpha$  and  $u$  can be estimated from the limited samples of the extreme value observations, i.e.,

$$m = \frac{\gamma}{\alpha} + u, \quad \gamma = 0.5772\text{-----} \quad (8)$$

$$\sigma = \frac{\pi}{\sqrt{6}} \frac{1}{\alpha} \quad (9)$$

Here  $m$  and  $\sigma$  are, respectively, the mean and standard deviation of the sample of extreme value observations.

Furthermore, Gumbel constructed a "probability paper" on which the extreme values of the air load obtained from  $N$  batches of data, each consisting of  $n$  observations are traced along the ordinate. The probability  $\Phi(x)$  and  $y$  are traced along the abscissa. The number of return period  $T(x)$  defined by

$$T(x) = \frac{1}{1 - \Phi(x)} \quad (10)$$

can be plotted along another scale parallel to  $\Phi(x)$ . Since in practical cases the number of extreme observations  $N$  is not infinity, the modification was made as follows.

$$\frac{1}{\alpha} = \frac{\sigma}{\sigma(N)} \quad ; \quad \lim_{N \rightarrow \infty} \sigma(N) \rightarrow \frac{\pi}{\sqrt{6}} \quad (11)$$

$$u = m - \frac{\bar{Y}(N)}{\alpha} \quad ; \quad \lim_{N \rightarrow \infty} \bar{Y}(N) \rightarrow \gamma \quad (12)$$

where  $\sigma(N)$  and  $\bar{Y}(N)$  are functions of  $N$  which was tabulated in Ref. 6.

The detailed summary of the theory can be found in Ref. 7.

### 3. APPLICATION OF THE FLUCTUATING AIR LOAD ACTING ON A CYLINDER

The experimental data on the fluctuating air load acting on a cylinder were taken from a thesis which was done by Robert E. Spitzer, (Ref. 4).

The experiment was mainly the recording of the fluctuating pressure and resultant forces from a smooth cylinder (8.54-inch diameter) cantilevered 8.1 diameters from a flat floor in the wind tunnel. The range of Reynolds number was  $2.5 \times 10^5 < Re < 7.5 \times 10^5$ .

Fluctuating pressures were measured through a 0.025-inch orifice by a reluctance-type pressure transducer. The angular position was determined by rotation of the model to align the orifices with a protractor to within one degree of the desired value. Proper back pressure was supplied to the transducer by a second orifice placed 0.75-inch below the transducer orifice at the same angular position. To obtain a steady back pressure, a calibrated "dashpot" was placed in the system to dampen the fluctuations in pressure from the back pressure orifice, and this static surface pressure was measured using a fluid-in-glass manometer.

Lift fluctuations were measured using the instrumented sections built by Schmidt. Lift was determined by 18 pressure transducers, nine on each side of the section, spaced to cover equal portions of the cylinder chord. Electrical integration of each nine gave the loading on each side of the cylinder. A differential 100 kc carrier amplifier gave the amplified electrical difference between the two sides, i. e., fluctuating lift signal.

The original data were recorded on the magnetic tape. Because a tremendous amount of data has to be handled, the records were converted to the digital form by using the Biological System Mark II Analog - Digital converter at Caltech Computing Center. The signal of the analog tape was sampled and converted to a binary number at a pre-selected timing rate, 500 samples per second, whereupon it is transferred to a digital tape via an input sub-channel in the IBM 7094 system; then a program was made according to the theory, to select the extreme values.

At each angular orientation of the cylinder in the flow and at a specific Reynolds number, the experiment has about 3 minutes of data in analogy form. The Analog-Digital converter converts them into the digital form by the rate of 500 samples per second; in other words, each experiment has 90,000 samples which are the input data of the computer program. The program was made to scan the input data and pick up the largest value among each 2500 samples in sequence. In other words, the extreme values are selected at each 5 second interval (2500 samples in digital form). Totally, about 36 extreme values are obtained for 3 minutes of data for every experiment. They are not necessarily the first 36 largest data among 90,000 samples, but they are the largest among the each 2500 samples as required by the theory. The time interval between each successive extreme values is also not necessarily 5 seconds, it can be any value between zero seconds and 10 seconds.

In worksheets 1 and 2, an example of lift coefficient (resultant force in the direction perpendicular to air flow) at Reynolds number  $7.5 \times 10^5$ , is given. Those extreme values  $x$  are picked up from the input data by the computer at 5 second intervals. These extreme values are arranged according to their magnitude in worksheet 1. Then the ordering number,  $\lambda$ , (here called the cumulative frequency) is assigned. The plotting position is then computed simply as  $\lambda/(N+1)$ ,  $N$  being the number of batches of data. (Notice that there are only 35 extreme values instead of 36; the last one in the digital tape was ruled out due to electronic noise.) Then the mean  $m$  and the standard deviation  $\sigma$  are calculated from the data according to worksheet 2. The parameters  $\alpha$  and  $u$  can be estimated according to Ref. 6, as shown in sheet 2. Figure 1 shows Gumbel's probability paper. The experimental data from worksheet 1 are plotted with the plotting position  $\lambda/N+1$  as abscissa and the corresponding  $x$  as ordinate. The theoretically estimated straight line relationship of the extreme distribution is calculated in worksheet 2 and plotted in Fig. 1.

The control curves, which represent 95% confidence level, are also plotted. The method of calculating such control curves is explained in detail in Ref. 6 and the results are shown in sheet 2.

In Tables 1 and 2, the parameters  $\alpha$  and  $u$  are listed for  $C_p$ , the pressure coefficient, and  $C_f$ , the coefficient of resultant force, for different Reynolds numbers and different angular orientations. ( $\theta = 0$  corresponds to the flow direction.)

It is clear now, by specifying the extreme value of the pressure or the force which can be withstood safely by the cylinder, one can calculate the probability of occurrence of that extreme value by means of eqs. (4) and (5). Then the length of the time interval in which such an extreme value is expected to occur once, multiplying the return period from eq. (10) with the time interval of observation, (e.g., 5 seconds in this case). Conversely, by specifying the lift of the structure, one can obtain the largest air load that will be encountered within this period.

#### 4. ENVELOPE OF EXTREME VALUES OF PRESSURE

If we specify the period that the cylinder will be exposed to the air flow to be 500 seconds, then the return period,  $T(x)$ , at 5-second intervals will be 100. In other words, the probability  $\Phi(x)$  is, by eq. (10),

$$\Phi(x) = 1 - \frac{1}{T} = 0.99$$

The reduced extreme value  $y$  can be obtained by eq. (4):

$$\Phi(x) = e^{-e^{-y}}$$

And then the largest value of the air load which the cylinder will encounter within 500 seconds can be obtained by eq. (5):

$$x = u + \frac{1}{\alpha} y$$

In Figures 2, 3, 4, 5, and 6, these largest pressure coefficients within 500 seconds were plotted for different Reynolds numbers and angular orientations.

It is necessary to emphasize that the extreme value curve did not represent any particular loading. They are the most probable values of air load the cylinder will encounter within 500 seconds. Therefore, the curve forms an envelope from which the largest expected value can be obtained. Clearly, this kind of information is of vital importance to the structure designer.

Now let us look at each figure individually. In Figure 2,  $Re = 2.5 \times 10^5$ . The  $C_p$  with the largest absolute value is negative

from  $\theta = 0^\circ$  (parallel to free stream) to  $\theta \approx 40^\circ$  and then becomes positive. The maximum  $C_p \approx 8.0$  occurs approximately at  $\theta = 100^\circ$ . Since the Reynolds number is not very high, a periodic structure in the pressure history was observed during the digitization through an oscilloscope. However, the signals were somewhat random.

The  $C_p$ 's are plotted with 95% confidence band. The extreme envelope is defined by a curve which traces along these  $C_p$ 's. Also the static pressures, which were measured by a fluid-in-glass manometer connected with an orifice on the cylinder surface, are plotted. The root-mean-square values of pressure, which were recorded by a Ballantine type 320 True RMS Voltmeter with capacitive damping to give a long time constant, are also plotted for comparison. The envelope shown in this picture cannot be predicted by only knowing the pressure is periodic.

Figures 3, 4, and 5 are for Reynolds number  $3.8 \times 10^5$ ,  $5.3 \times 10^5$  and  $6.5 \times 10^5$ , respectively. One can see there are two peaks in each extreme value envelope. One is at  $\theta = 10^\circ$  which is the smaller one, the other is at  $\theta = 100^\circ$ , which is the maximum extreme value. Comparing these two peaks with static pressure which is also plotted by dotted lines, it seems that there is a phase shift, since the two largest static  $C_p$ 's are at  $\theta = 0^\circ$  and  $\theta = 80^\circ$ . Two phenomena are observed: one is that all extreme values are negative. The other is that the peak values are decreasing with increasing Reynolds number. In other words, that the largest pressure is not necessary happened for the largest Reynolds number.



Once again if we compare the extreme value envelope with the static pressure, the former is considerably greater than the latter.

In Fig. 6, for Reynolds number  $7.5 \times 10^5$ , the peak at  $\theta = 80^\circ$  seems to be in phase with that of the static pressure. The signals observed during the digitizing were highly random. However, the extreme values are smaller than that of the smaller Reynolds number.

The extreme values in Figs. 2, 3, 4, 5 and 6 have the return period of 100, corresponding to a time interval of 500 seconds. In other words, the probability is 0.99 for the cylinder to encounter such an extreme air load in every 500 seconds. It is understood, however, if we specify a different probability or a different return period, different extreme values will be obtained.

## 5. ENVELOPE OF EXTREME VALUE OF RESULTANT FORCE

Spitzer also presented the measurements of the forces acting on the cylinder induced by the flow. The measurements were made for different Reynolds numbers and in different directions from  $90^\circ$  to  $270^\circ$  with respect to the air stream. Usually the resultant force in the direction of  $\theta = 90^\circ$  is called the drag. In this report the resultant forces in other directions are also examined.

The technique explained in the previous section has been applied also to the resultant force. Fig. 7 shows the extreme value of the coefficient of the resultant force in a period of 500 seconds.  $\theta$  denotes the direction of force with respect to the air stream.

$C_f = \frac{F}{q}$  is the force coefficient, where  $q$  is dynamic pressure.

As before, the envelope of the extreme resultant force does not represent any particular loading at a given instant of time. The envelope represents the most probable largest force the cylinder will encounter once in 500 seconds. Once again we notice that larger Reynolds number does not give larger force. The envelope was drawn for all different Reynolds numbers from  $2.5 \times 10^5$  to  $7.5 \times 10^5$ . Obviously, such an extreme value envelope is useful for design purposes.

## 6. EFFECT OF THE VARIATION OF THE SAMPLING TIME INTERVAL

There are two questions left to be answered. One is whether the extreme value distribution is strongly influenced by the time interval of data collection. The other is whether the initial distribution is exponential. To examine the first question, the resultant forces in  $\theta = 90^\circ$  (lift) and  $\theta = 180^\circ$  (drag) for a period of 500 seconds were analyzed. The lift and drag coefficient are plotted versus different sampling time intervals in Fig. 8. The different sampling time interval seems to have no effect on the extreme values. Therefore, the extreme value can be picked up by any convenient interval as long as the flow condition remains unchanged.

## 7. DISCUSSION

Since Gumbel's extreme-value theory is based on the initial distribution being of an exponential type, it is necessary to examine the initial distribution by an extensive data collection and analysis. However, if we assume that 87,500 observations did represent a large sample, then the initial distribution can be obtained by usual means. A computer program was made to do this. The data used was absolute value of the lift coefficient (corresponding to the resultant force in the direction perpendicular to the free stream). The analysis shows that this distribution has a mean value of 0.629 and a standard deviation of  $\sigma = 0.40404$ . The frequency function is plotted in Fig. 9. The experimental data may be compared with the normal distribution with the same mean and standard deviation as shown in the figure. However, one must realize that since the variate  $|C_L|$  is positive, its distribution cannot be normal even if  $C_L$  itself is normally distributed. The comparison therefore is incomplete, but is offered for future examinations.

The experimental data used in this report were only from one section of the cylinder where the instrumentation was placed. It is obvious that for a cantilever cylinder of finite length the fluctuating air loads will vary from one end to another. Refs. 9, 10, and 11 deal with this three-dimensional effect extensively, but inconclusively. No detailed study of the extreme pressure variation along a three-dimensional body has been made. Evidently much remains to be done in this field.

## 8. CONCLUSION

Gumbel's extreme value theory has been applied to many problems such as the effective gust velocity and the extreme wind-speed (Ref. 8) and was proved adequate. This report shows that the same theory is useful in the problem of predicting the fluctuating air load acting on a cylinder in a flow at large Reynolds number. The varied relationships between the extreme value envelope and the static and the root-mean-square curves are demonstrated in this report. It is shown that there are considerable differences between the static air load distribution and extreme air load distribution. This information should be useful in practical design of cylindrical structures.

From Figures 2-6, it is seen that the extreme value envelope is not entirely similar to the root-mean-square curve for the pressure distribution around the circumference. Therefore the current practice of estimating the extreme value by multiplying the root-mean-square values with a uniform constant (say  $3\sigma$ ) cannot be a rigorously valid procedure. However, in all the cases examined, the position around the circumference when the largest extreme value of pressure occurs seems to coincide with the point when the largest root-mean-square value occurs.

## 9. REFERENCES

1. Fung, Y. C., "The Analysis of Wind-Induced Oscillations at Large and Tall Cylindrical Structures", Space Technology Laboratories, Inc., STL/TR-60-0000-09134, EM10-3 (June 1960).
2. Fung, Y. C., "Fluctuating Lift and Drag Acting on a Cylinder in a Flow at Supercritical Reynolds Numbers", Journal of Aerospace Sciences, Vol. 27, No. 11, pp. 801-814. (November 1960).
3. Schmidt, L. V., "Measurement of Fluctuating Air Loads on a Circular Cylinder", Ph. D. Thesis, California Institute of Technology (1963).
4. Spitzer, R. E., "Measurements of Unsteady Pressure and Wake Fluctuations for Flow over a Cylinder at Supercritical Reynolds Number", A.E. Thesis, California Institute of Technology (1965).
5. Cramer, H., "Mathematical Methods of Statistics", Princeton University Press, 1946, pp. 370-378.
6. Gumbel, E. J., "Statistics of Extremes", Columbia University Press, New York, 1958.
7. Chen, J. C., "Study of Theory of Extreme Values and an Application of Air Load to Cylinder", preliminary report of Aeroelasticity and Structural Dynamics. California Institute of Technology, September 1965.
8. Gumbel, E. J., and Carlson, P. G., "Extreme Values in Aeronautics", Journal of Aeronautical Sciences, Vol. 21, No. 6, pp. 389, June 1954.
9. Blackiston, H. S., "Tip Effects on Fluctuating Air Loads on a Circular Cylinder", AIAA Fifth Annual Structures and Materials Conference, pp. 146, April 1964.
10. Rainey, G. A., "Progress on the Launch-Vehicle Buffeting Problem", AIAA Fifth Annual Structures and Materials Conference, pp. 163, April 1964.
11. Buell, D. A., "Some Sources of Ground-Wind Loads in Launch Vehicles", AIAA Fifth Annual Structures and Materials Conference, pp. 178, April 1964.

PROBABILITIES OF EXTREMES

Worksheet 1

<u>Cumulative Frequency</u>	<u>Extremes</u>	<u>Extreme Square</u>	<u>Plotting Position</u>
$\lambda$	x	$x^2$	$\frac{\lambda}{N+1}$
1	1.853	3.433	0.0278
2	1.859	3.457	.0556
3	1.875	3.517	.0833
4	1.885	3.553	.1112
5	1.904	3.626	.1389
6	1.933	3.737	.1667
7	1.952	3.812	.1944
8	1.994	3.976	.2222
9	1.994	3.976	.2500
10	2.013	4.051	.2778
11	2.017	4.066	.3056
12	2.033	4.131	.3333
13	2.033	4.131	.3611
14	2.038	4.155	.3889
15	2.039	4.158	.4167
16	2.097	4.397	.4444
17	2.110	4.451	.4722
18	2.110	4.451	.5000
19	2.116	4.478	.5278
20	2.119	4.491	.5556

PROBABILITIES OF EXTREMES

Worksheet 1 (continued)

<u>Cumulative Frequency</u>	<u>Extremes</u>	<u>Extreme Square</u>	<u>Plotting Position</u>
$\lambda$	$x$	$x^2$	$\frac{\lambda}{N+1}$
21	2.129	4.532	.5833
22	2.145	4.601	.6111
23	2.148	4.615	.6389
24	2.158	4.656	.6667
25	2.161	4.670	.6944
26	2.180	4.754	.7222
27	2.212	4.895	.7500
28	2.225	4.952	.7777
29	2.306	5.315	.8056
30	2.312	5.345	.8333
31	2.373	5.631	.8611
32	2.447	5.987	.8889
33	2.482	6.161	.9167
34	2.489	6.193	.9444
35	2.643	6.983	.9722
Sum:	$N = \underline{35}$	$\Sigma X_i = \underline{74.3826}$	$\Sigma X_i^2 = 159.3353$



PROBABILITIES OF EXTREMES

Worksheet 2

I. Mean and Standard Deviation:

$N = \underline{35}$                        $\Sigma X_i = \underline{74.3826}$                        $\Sigma X_i^2 = \underline{159.3353}$   
 Mean  $\bar{X} = 2.125$                       Standard Deviation  $S_x = \underline{0.18946}$

II. Parameters:

$\sigma_N = \underline{1.12847}$                        $\bar{Y}_N = \underline{0.54034}$                        $\frac{1}{\alpha} = \frac{S_x}{\sigma_N} = \underline{0.16789}$

$\frac{1}{\alpha} \bar{Y}_N = \underline{0.09072}$                        $U = \bar{X} - \frac{1}{\alpha} \bar{Y}_N = \underline{2.0345}$

III Line of Expected Extremes:

$X = U + \frac{1}{\alpha} y = \underline{2.0345} + \underline{0.16789} y$

y:	<u>-2.00</u>	<u>0.00</u>	<u>2.25</u>	<u>3.00</u>	<u>4.60</u>	<u>5.00</u>
	<u>.000618</u>	<u>.36787</u>	<u>.9000</u>	<u>.95143</u>	<u>.9900</u>	<u>.99328</u>
T	<u>1.0006</u>	<u>1.582</u>	<u>10.</u>	<u>20.589</u>	<u>100.</u>	<u>148.81</u>
$\frac{1}{\alpha} y$	<u>-0.3358</u>	<u>0.0</u>	<u>0.3778</u>	<u>0.5037</u>	<u>0.7723</u>	<u>0.8394</u>
X	<u>1.6987</u>	<u>2.0345</u>	<u>2.4123</u>	<u>2.5382</u>	<u>2.8068</u>	<u>2.8739</u>

IV. Control Curve (0.68269 Confidence Band)  $\frac{1}{\sqrt{\alpha}} N = \underline{0.02838}$

$\sigma_{x,m} = \sigma_{y,m} N / (\alpha N)$

	.15	.20	.30	.40	.50	.60	.70	.80	.85
$\sigma_{y,m} N$	1.225	1.245	1.268	1.337	1.443	1.598	1.835	2.241	2.585
$\sigma_{x,m}$	<u>0.03476</u>	<u>.03533</u>	<u>.03598</u>	<u>.03794</u>	<u>.04095</u>	<u>.04535</u>	<u>.05207</u>	<u>.06360</u>	<u>.07336</u>

For largest value  $\Delta_{x,N} = 1.141 \left(\frac{1}{\alpha}\right) = \underline{0.19156}$

For next to largest value  $\Delta_{x,N-1} = .759 \left(\frac{1}{\alpha}\right) = \underline{0.12743}$

TABLE I

Parameters for Pressure Coefficient

Re =		2.5x10 <sup>5</sup>	3.8x10 <sup>5</sup>	5.3x10 <sup>5</sup>	6.5x10 <sup>5</sup>	7.5x10 <sup>5</sup>
$\theta$	q	5 psf	10 psf	20 psf	30 psf	40 psf
0°	u	-0.9131	-6.1213	-3.1293	-0.2405	+3.1158
	1/α	-0.3944	-0.0626	-0.0246	-0.01978	+0.1242
10°	u	-1.1814	-9.4193	-8.2690	-6.0943	-3.0790
	1/α	-0.9599	-0.3663	-0.0439	-0.0995	0.1065
20°	u	+3.9001	-4.4404	-7.1309	-5.0060	-2.3902
	1/α	+0.9976	-0.3616	-0.0756	-0.1056	-0.0466
30°	u	-1.9215	-5.2340	-3.5880	-2.3738	-0.8098
	1/α	-0.4151	-0.1507	-0.1269	-0.0912	-0.2065
40°	u	-1.7117	-4.0034	-3.0587	-2.6545	-1.4811
	1/α	-0.5060	-0.1777	-0.0745	-0.0917	-0.0348
50°	u	+1.3555	-3.4934	-5.2368	-5.0609	-3.5406
	1/α	+0.2862	-0.3566	-0.1072	-0.0216	-0.1558
60°	u	+3.2109	-3.5628	-5.3074	-5.8657	-5.2192
	1/α	+0.3347	-0.3738	-0.1416	-0.0479	-0.1312
70°	u	+4.3306	-3.9345	-6.8682	-7.0183	-6.2664
	1/α	+0.5898	-0.6569	-0.1485	-0.0801	-0.1300
80°	u	-6.8368	-5.9694	-5.9361	-5.2165	+0.4327
	1/α	-0.5690	-0.1958	-0.1105	-0.1469	+0.1999
90°	u	+4.2214	-6.1723	-7.8781	-7.7787	-6.6232
	1/α	+0.3909	-0.5378	-0.1680	-0.1174	-0.1456
100°	u	+5.2784	-4.3065	-6.7680	-7.3900	-6.1738
	1/α	+0.5654	-0.4964	-0.2066	-0.2037	-0.1864
110°	u	-3.4521	-14.4222	-9.9789	-7.9259	-4.5334
	1/α	-0.9694	-0.9837	-0.7127	-0.4194	-0.0578
120°	u	+6.3648	-7.1614	-8.4080	-8.3555	-5.5783
	1/α	+0.1705	-0.7087	-0.2751	-0.1565	-0.0011
130°	u	+6.2374	-3.3111	-6.2858	-7.0644	-5.4340
	1/α	+0.5702	-0.4375	-0.2819	-0.4607	-0.0690
140°	u	-4.4586	-4.1552	-6.0659	-5.5716	-3.3114
	1/α	-0.9040	-0.3275	-0.1981	-0.1761	-0.0146
150°	u	+3.8734	-2.2766	-4.8023	-5.3958	-3.9431
	1/α	+0.4860	-0.4642	-0.0972	-0.2086	-0.0082
160°	u	+4.1663	-1.7394	-3.1137	-3.9476	-3.0792
	1/α	+0.5650	-0.2504	-0.1185	-0.1746	-0.1548
180°	u	+4.3366	+3.2137	-3.1710	-4.1549	-3.1775
	1/α	+0.4359	+0.1645	-0.1753	-0.1583	-0.1264

TABLE 2

Parameters for Pressure Coefficient

$\theta$	$q$	5 psf	10 psf	20 psf	30 psf	40 psf
0°	u	1.8101		3.4304	2.3315	2.0345
	1/α	0.22		0.2985	0.6164	0.1679
10°	u	1.552	1.6849	3.2345	3.0233	2.2559
	1/α	0.33	0.2842	0.2247	0.2595	0.3438
20°	u	1.6664	1.0185	1.3842	2.3721	2.2777
	1/α	0.4363	0.2689	0.1198	0.1801	0.2613
30°	u	1.6075	2.4458	2.8774	3.0083	2.5393
	1/α	0.2110	0.2309	0.2779	0.2059	0.1941
40°	u	1.6488	1.1337	2.0709		1.9781
	1/α	0.2882	0.0980	0.2499		0.2523
50°	u	2.6523	2.2969	2.3938		1.9604
	1/α	0.3869	0.1545	0.2773		0.2869
60°	u	2.0058	2.0135	2.0491	2.0916	1.9622
	1/α	0.2998	0.2417	0.2737	0.1448	0.2915
70°	u	1.9229		2.0228	2.1820	2.0787
	1/α	0.2418		0.3467	0.2473	0.2621
80°	u	1.9196	1.9858	2.1298	2.1976	2.1712
	1/α	0.2679	0.2306	0.2467	0.2145	0.1421
90°	u	2.9163	2.3070	1.8703	1.8653	2.4479
	1/α	0.1952	0.2250	0.1234	0.2020	0.2992
100°	u	1.5929	1.6991	2.4588	2.8840	2.6291
	1/α	0.2603	0.0883	0.2385	0.2499	0.3057
110°	u	1.7001	1.2474	2.9202	2.7987	1.9520
	1/α	0.2300	0.1064	0.3032	0.2334	0.2588
120°	u	1.7044	1.5375	2.2248	3.3287	3.0010
	1/α	0.3389	0.1351	0.2522	0.2334	0.2392
130°	u	1.4922	1.0968	2.2821		2.1825
	1/α	0.2468	0.1014	0.3894		0.2512
140°	u	1.7290	1.0273	2.0011	2.3040	2.0135
	1/α	0.2685	0.0927	0.2600	0.3057	0.3073
150°	u	2.9045	2.4157	2.5993	2.1009	2.1177
	1/α	0.3368	0.1245	0.3139	0.1990	0.2689
160°	u	1.7020	2.4857			2.2709
	1/α	0.3521	0.2718			0.2287
180°	u	1.8382	1.2238	2.0899		2.2545
	1/α	0.3168	0.1244	0.2645		0.2577

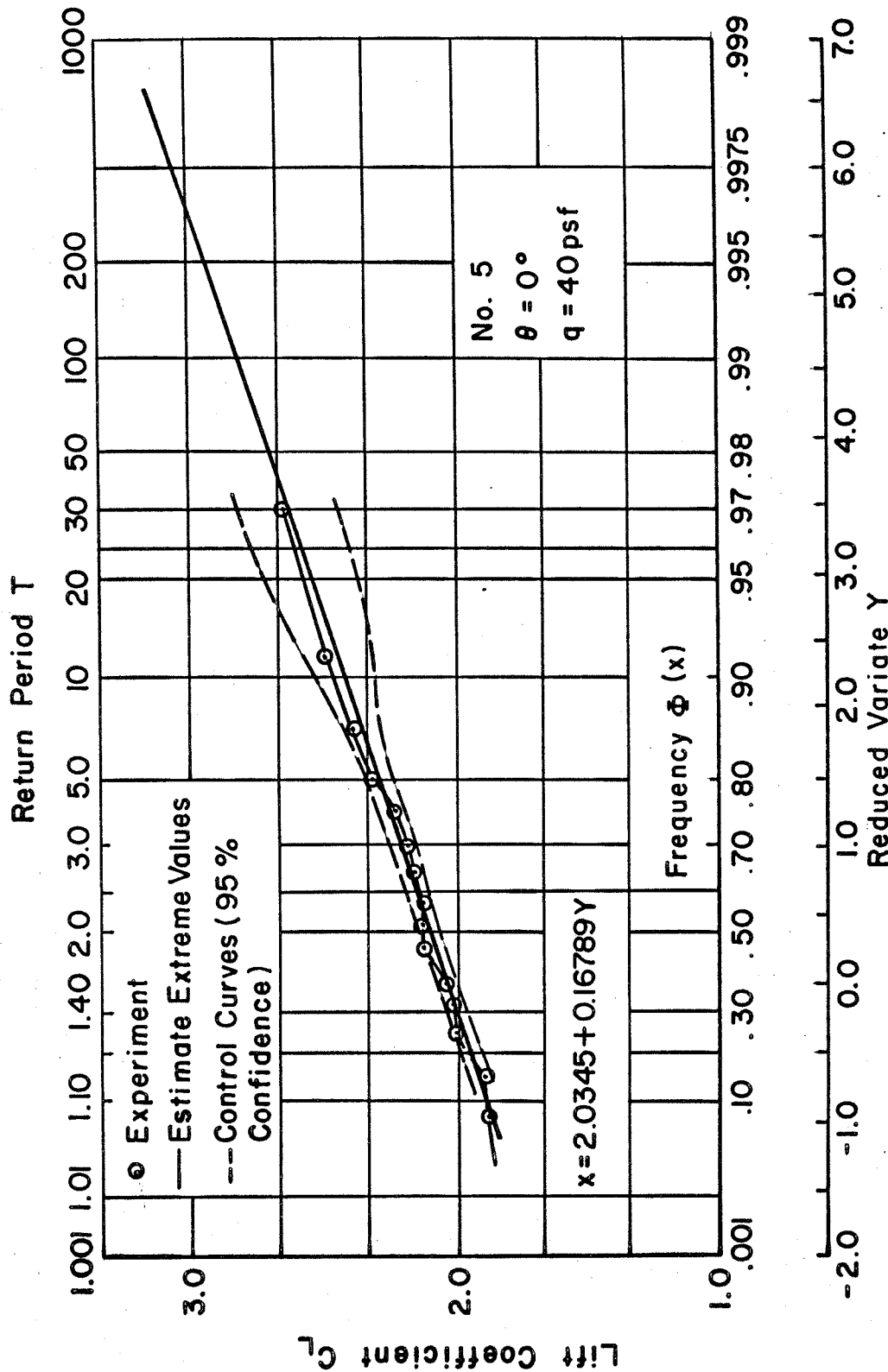


Figure 1. Probability Paper

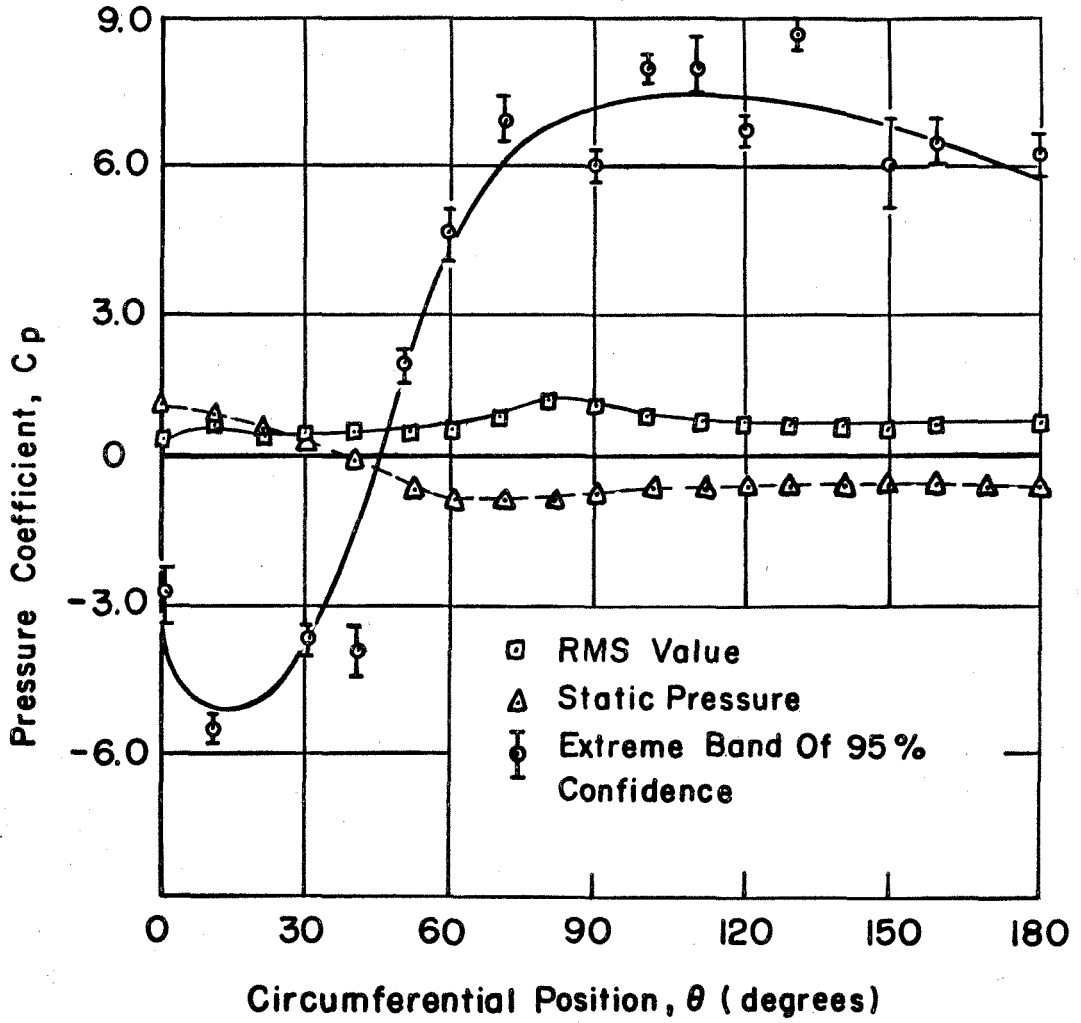


Figure 2. Extreme Envelope of  $C_p$ .  $Re=2.5 \times 10^5$

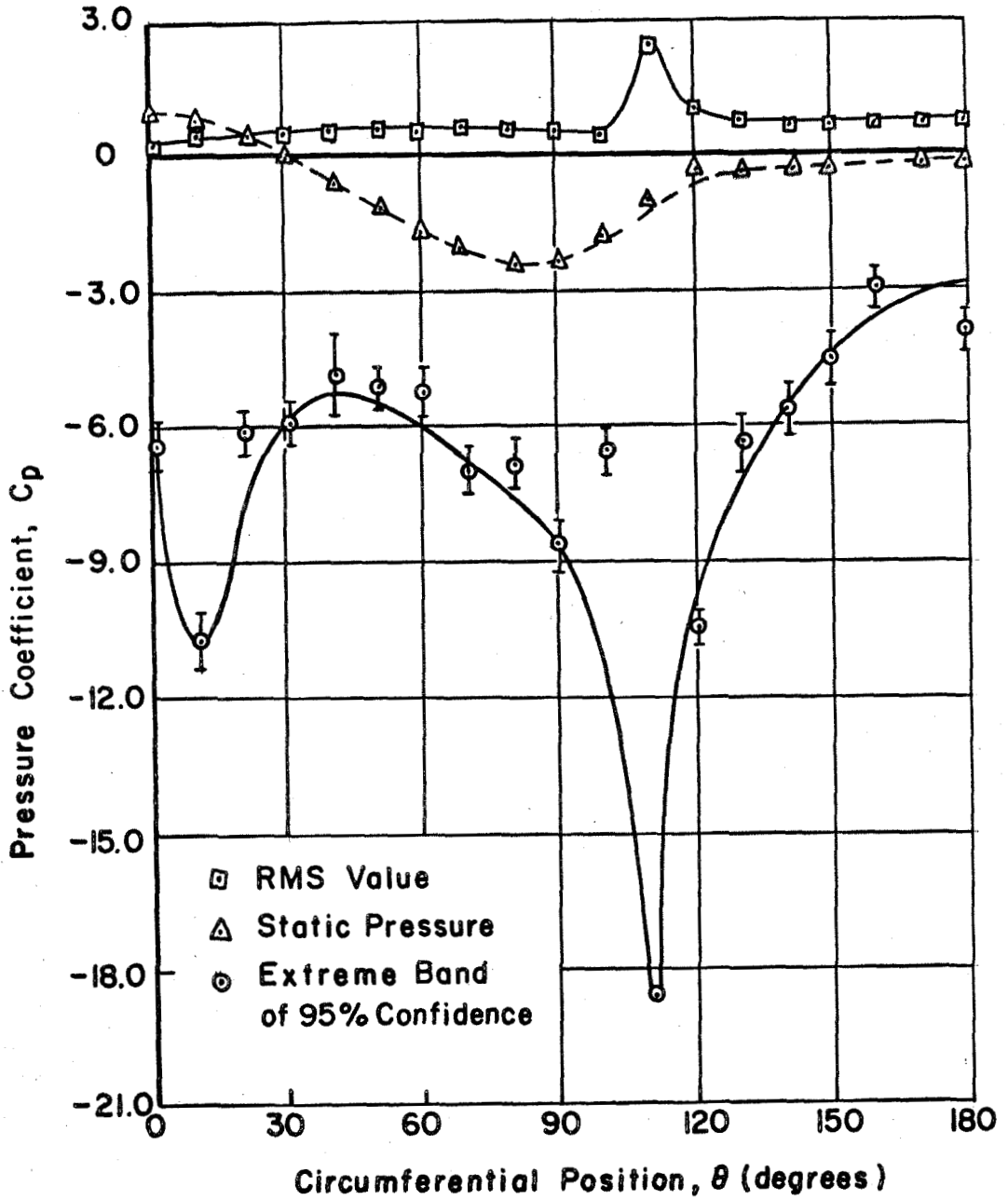


Figure 3. Extreme Envelope of  $C_p$ .  $Re=3.8 \times 10^5$ .

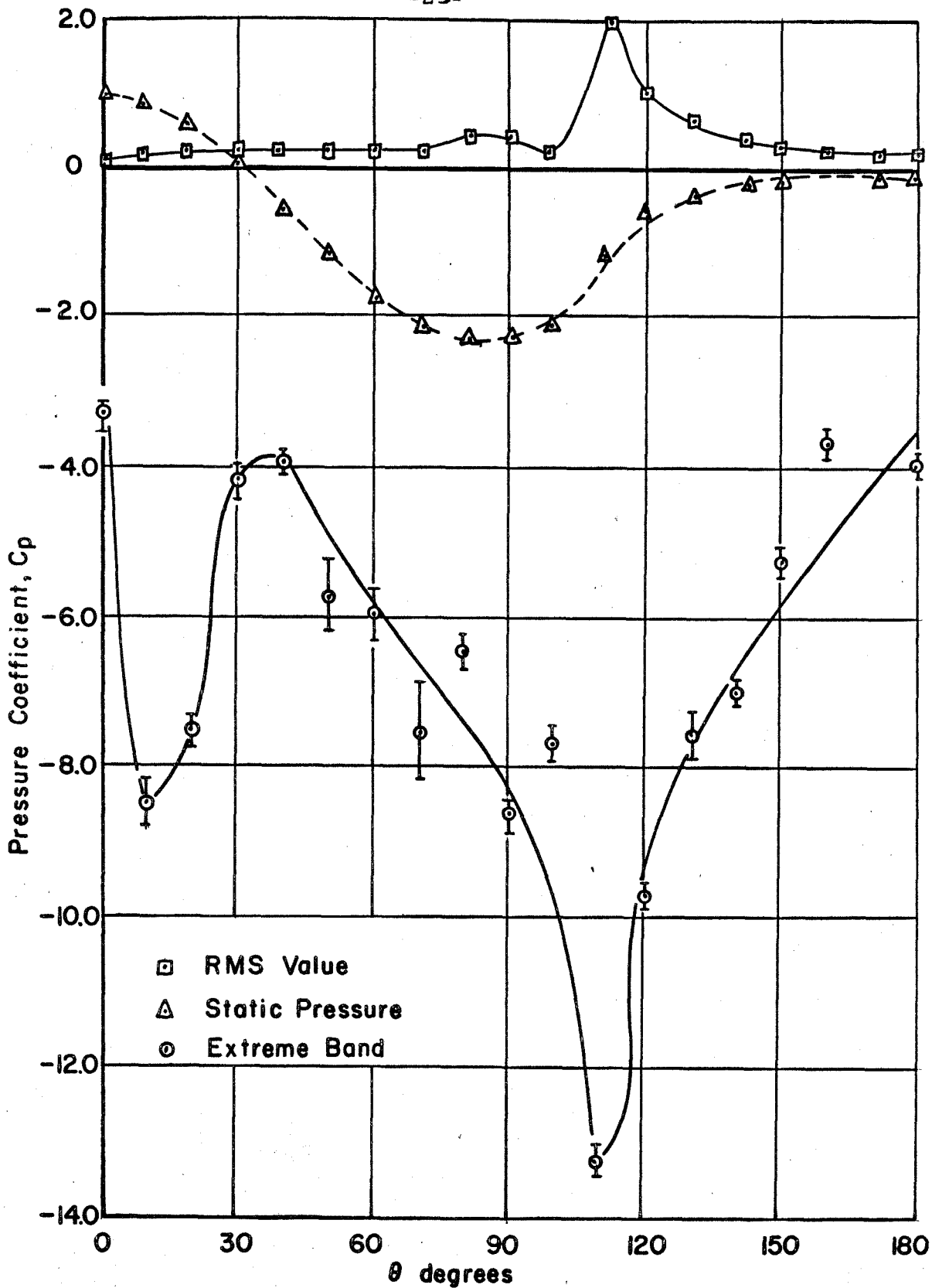


Figure 4. Extreme Envelope of  $C_p$   $Re = 5.3 \times 10^5$

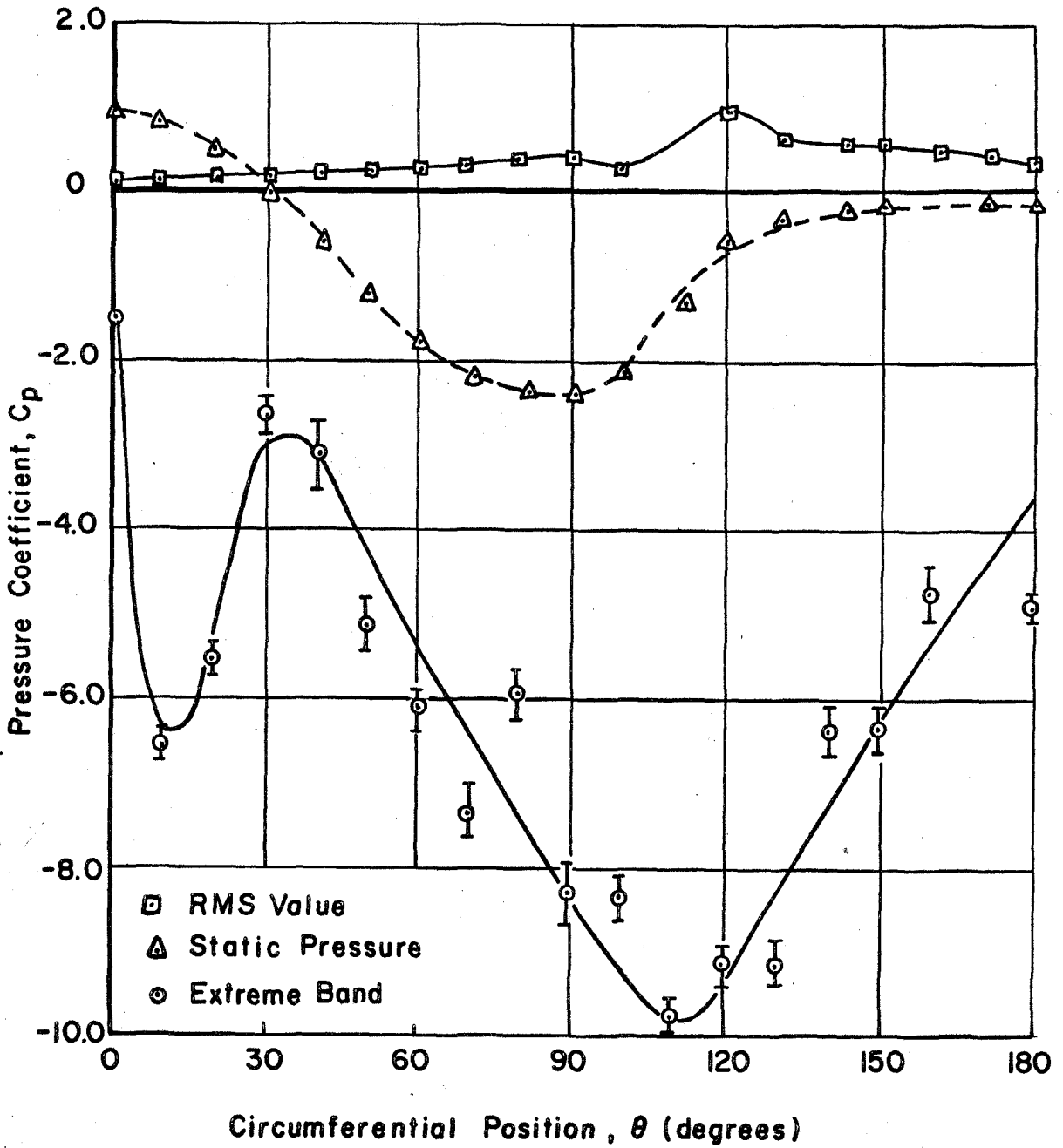


Figure 5. Extreme Envelope of  $C_p$   $Re = 6.5 \times 10^5$



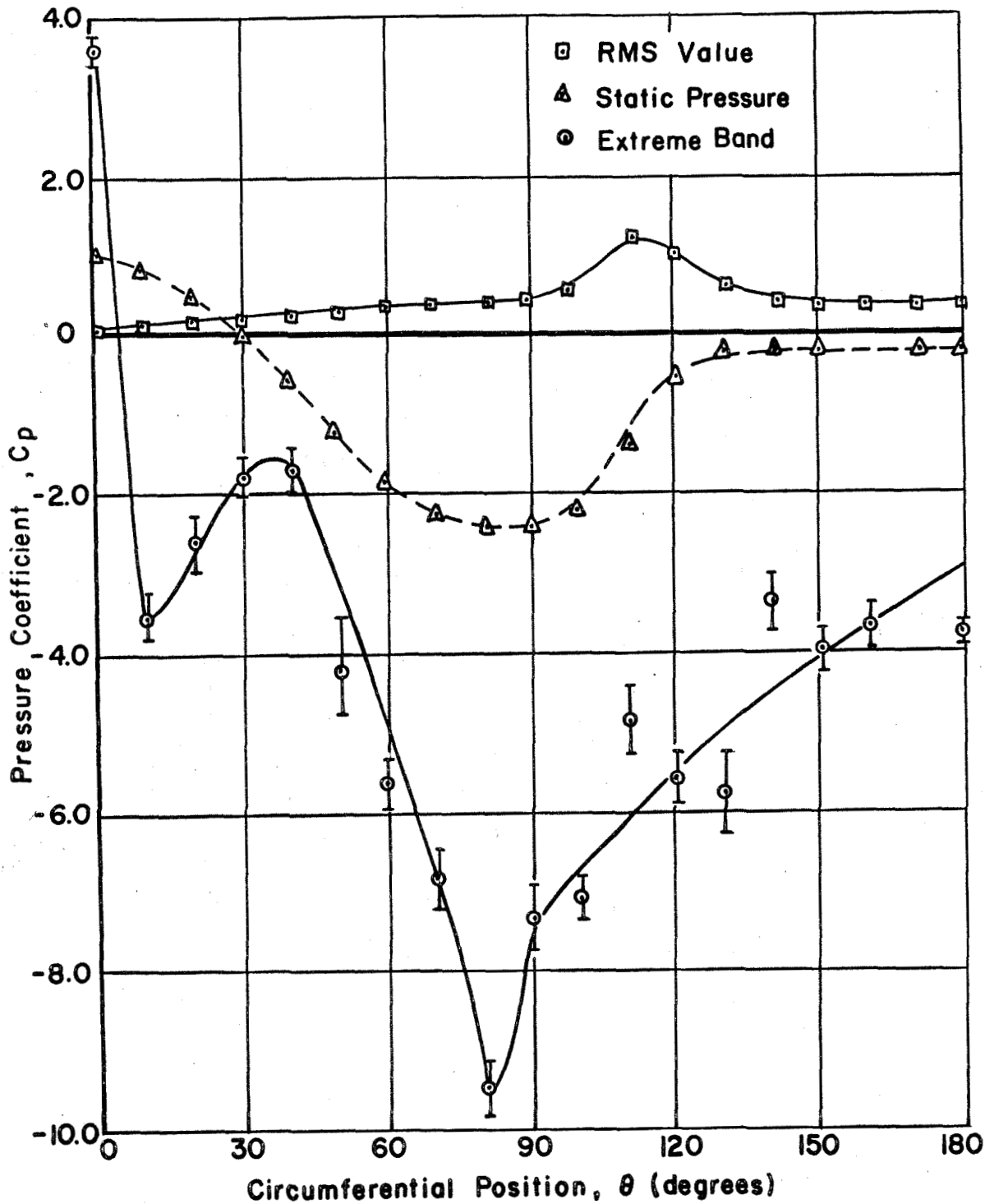


Figure 6. Extreme Envelope of  $C_p$   $Re = 7.5 \times 10^5$

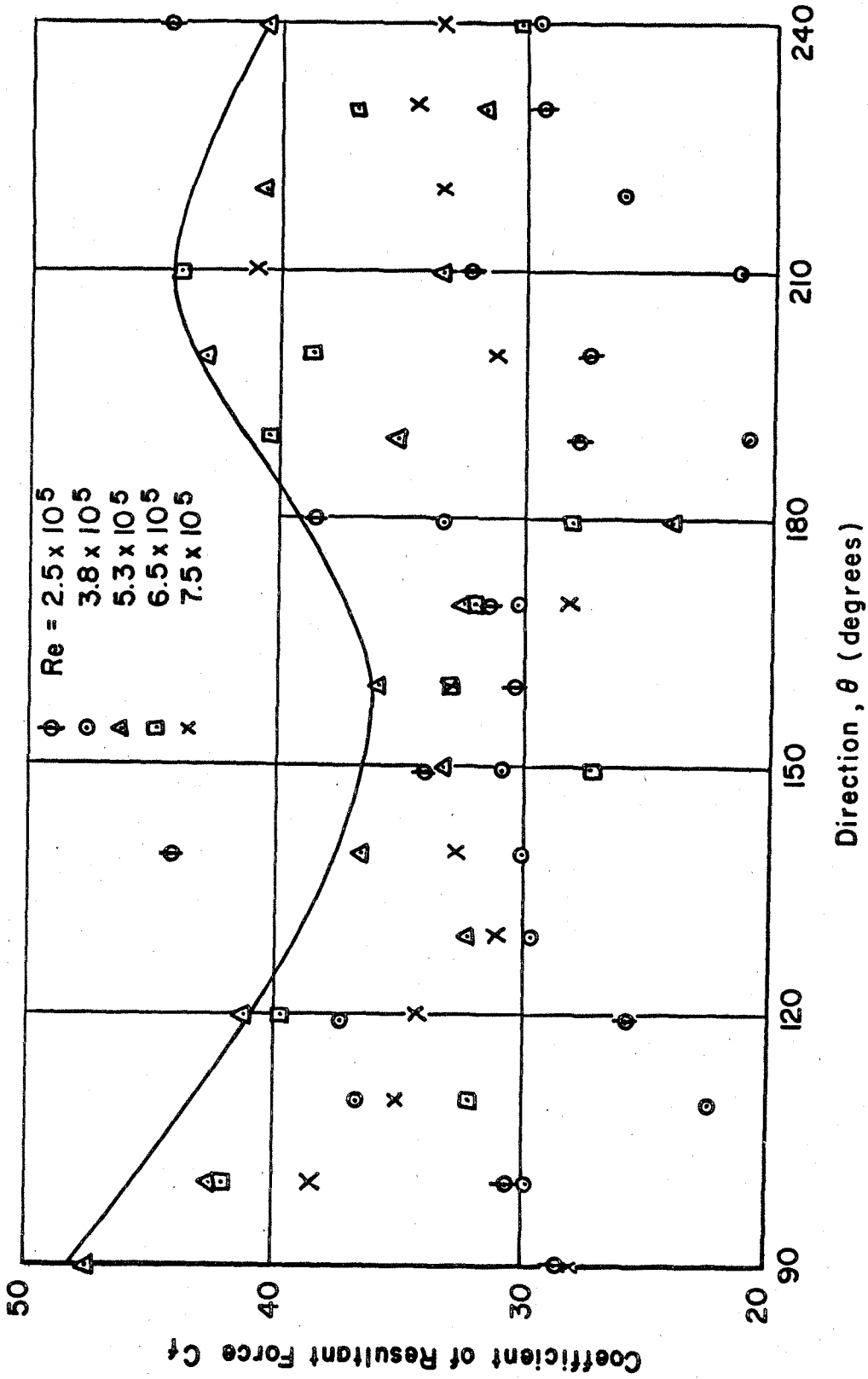


Figure 7. Extreme Envelope of  $C_f$

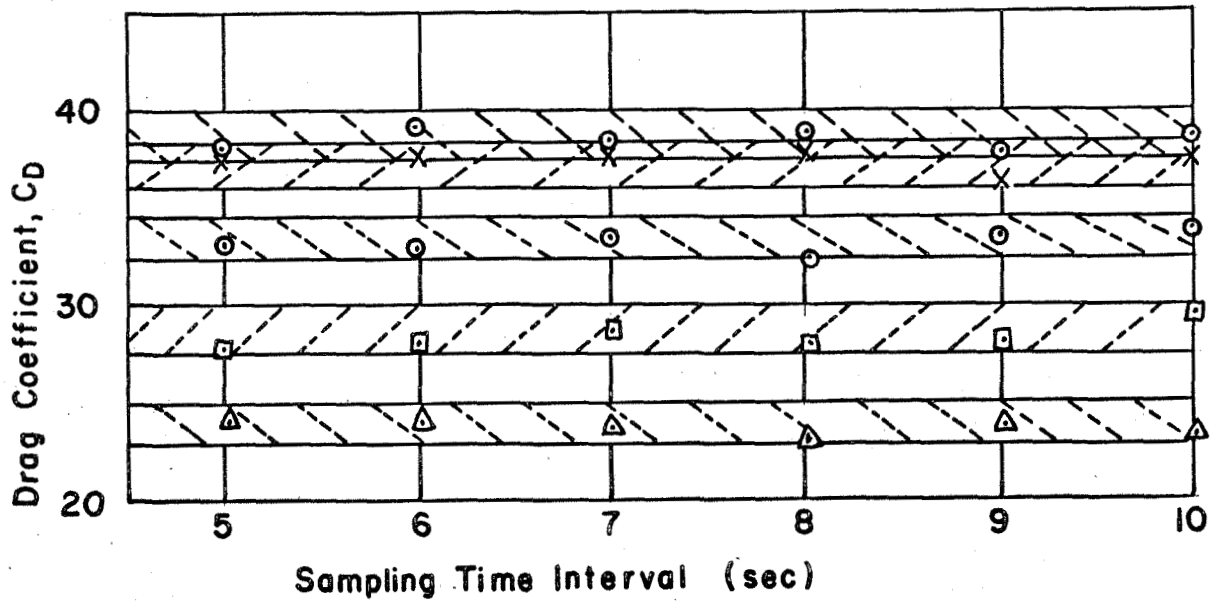
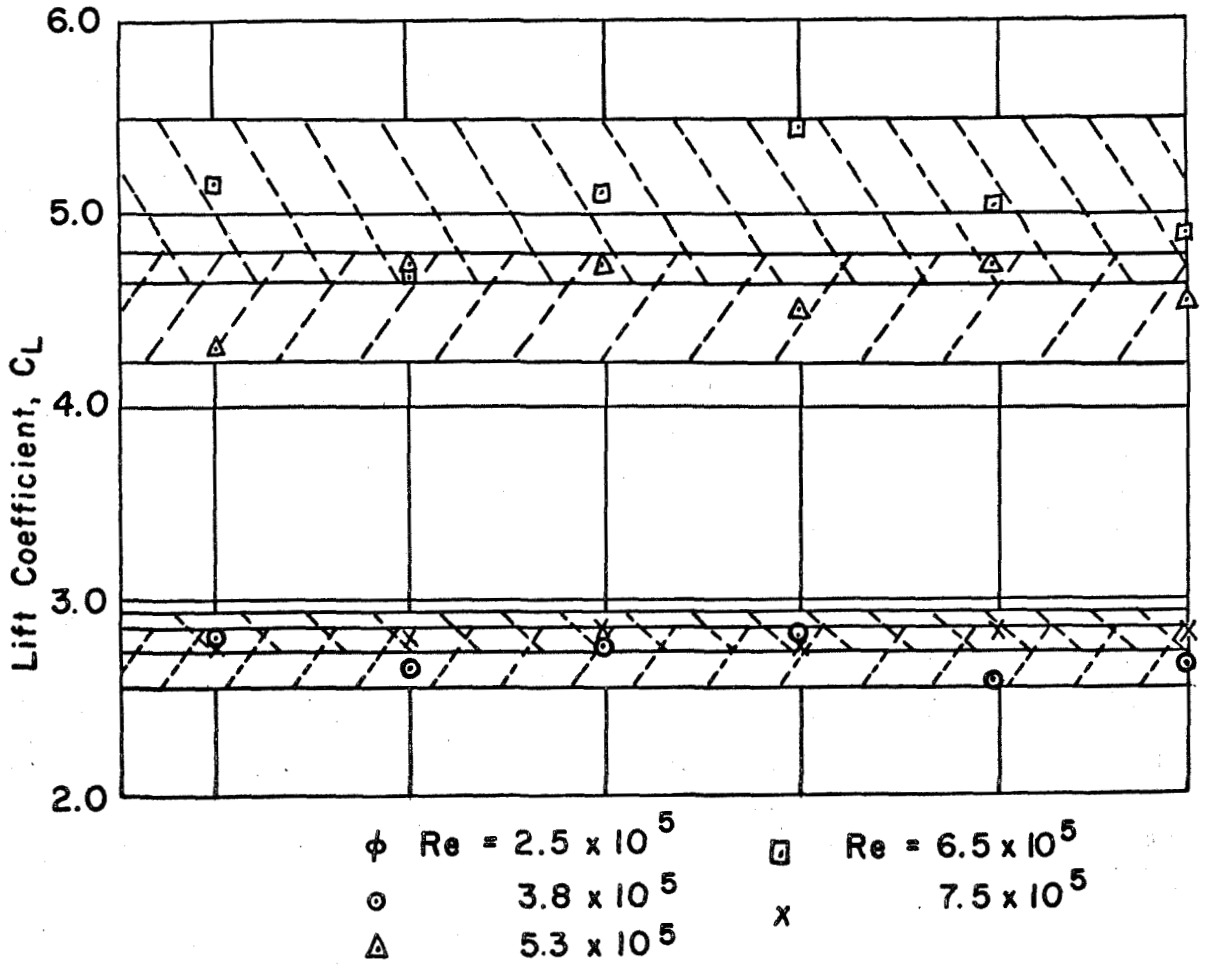


Figure 8. Extreme Interval V.S.  $C_L$  and  $C_D$

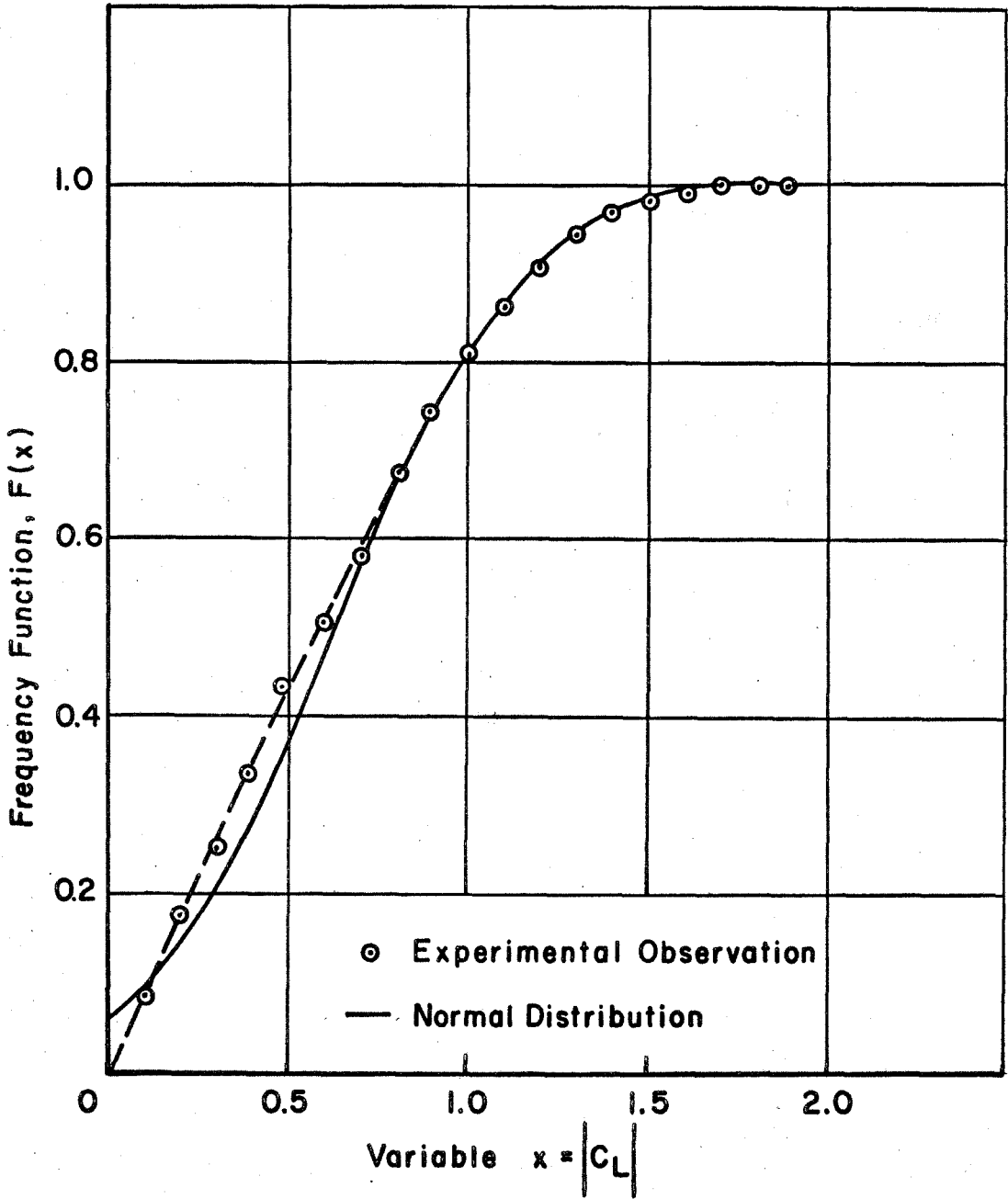


Figure 9. Initial Distribution